

Solving the dynamical mean-field theory at very low temperatures using the Lanczos exact diagonalization

Massimo Capone

SMC, CNR-INFM, and Dipartimento di Fisica, Università di Roma, "La Sapienza," piazzale Aldo Moro 5, I-00185 Roma, Italy and ISC-CNR, Via dei Taurini 19, I-00185 Roma, Italy

Luca de' Medici* and Antoine Georges

Centre de Physique Théorique, École Polytechnique, 91128 Palaiseau Cedex, France

(Received 7 August 2007; published 17 December 2007)

We present an efficient method to solve the impurity Hamiltonians involved in dynamical mean-field theory at low but finite temperature based on the extension of the Lanczos algorithm from ground state properties alone to excited states. We test the approach on the prototypical Hubbard model and find extremely accurate results from $T=0$ up to relatively high temperatures up to the scale of the critical temperature for the Mott transition. The algorithm substantially decreases the computational effort involved in finite temperature calculations.

DOI: [10.1103/PhysRevB.76.245116](https://doi.org/10.1103/PhysRevB.76.245116)

PACS number(s): 71.27.+a, 71.10.Fd, 71.30.+h

I. INTRODUCTION

Strongly correlated electron systems have received a great deal of attention in the past 20 years, owing to the interest in classes of materials such as high temperature superconductors or heavy fermions. Some of the striking properties of these materials such as strong mass renormalizations, Mott insulating phases, or unconventional magnetic properties are clearly due to the correlation between electrons, an aspect ignored, or poorly taken into account in conventional band theories. This has led to the development of an entirely new field and of new theoretical schemes and techniques. Among those, dynamical mean-field theory¹ (DMFT) has emerged as one of the most powerful, both for model Hamiltonians and as a way to take correlations into account in realistic electronic structure calculations.²

Within DMFT, spatial correlations are frozen, while local quantum dynamics is fully preserved, as it happens in the infinite coordination limit, where DMFT becomes indeed the exact theory. Under this approximation, a lattice model finds an effective description in terms of an impurity model in which an interacting site hybridizes with an effective bath of free electrons. The mapping onto the impurity model is enforced by a self-consistency condition³ which contains the information about the original lattice. The self-consistency equation, as we will see, connects the hybridization function of the impurity model to the local Green's function. Therefore, we can solve a lattice model within DMFT once we are provided with a method to solve the impurity model and compute the Green's function. The Anderson impurity model (AIM), albeit much easier to solve than the original lattice model, is still a nontrivial many-body problem whose solution requires either approximations or the use of numerical methods. Both "exact" numerical methods [exact diagonalization (ED),⁴ quantum Monte Carlo⁵ (QMC), and the recently introduced continuous-time version,⁶ numerical renormalization group⁷ (NRG), etc.] and approximate "analytical" methods (iterated perturbation theory,³ the noncrossing approximation⁸ and its slave-rotor extensions,⁹ the self-

energy functional method,¹⁰ and others) have been successfully employed. However, most methods have limitations confining them to either a specific regime (e.g., high temperatures) or to the investigation of specific physical aspects (e.g., low-energy quantities). In particular, focusing on numerical methods, Hirsch-Fye QMC is well suited for relatively high temperatures (and weak to intermediate correlations), while ED based on the Lanczos method has been up to now used only for $T=0$. The NRG, which uses Wilson's scheme to solve the AIM,⁷ is perfectly suited for an extremely accurate determination of the low-energy part of the spectra at zero temperature, but it is slightly less accurate on the high-energy part of the spectrum and for finite temperatures. There is no established reliable tool to deal with the regime of finite but very low temperature, which is particularly relevant in correlated systems in which very small energy scales arise, leading to subtle effects (such as spectral weight transfers) when the temperature is turned on. The aim of this paper is to introduce a simple modification of the Lanczos strategy in order to treat the low-temperature regime accurately and with a reasonable numerical effort. We emphasize that our approach is different from the finite-temperature Lanczos method developed by Jaklic and Prelovsek¹¹ and Aichhorn *et al.*,¹² which is built as a tool to use ED at any temperature, but it is in principle exact only at $T=0$ and in the large temperature limit. Our method is instead designed to treat the very low-temperature regime with the same accuracy of $T=0$, while it cannot be pushed beyond some model-dependent temperature without spoiling the rapidity of the Lanczos algorithm and thus without almost recovering the computational heaviness of the full diagonalization of the Hamiltonian.

As we anticipated, the DMFT method maps a lattice model onto an effective impurity model that we can write as

$$H_{\text{AIM}} = \sum_{l\sigma} \varepsilon_{l\sigma} a_{l\sigma}^\dagger a_{l\sigma} + \sum_{l\sigma} V_{l\sigma} (f_\sigma^\dagger a_{l\sigma} + a_{l\sigma}^\dagger f_\sigma) + H_{\text{at}}. \quad (1)$$

In this expression, f_σ^\dagger and $a_{l\sigma}^\dagger$ are creation operators for fermions in with spin σ associated with the impurity site and

with the state l of the effective bath, respectively. For simplicity, we consider a single band model, but the formalism is easily extended to multiorbital models. H_{at} is the on-site (atomic) part of the original lattice Hamiltonian, which contains the interaction terms. For the Hubbard model, $H_{\text{at}} = \varepsilon_f(n_f^{\uparrow} + n_f^{\downarrow}) + U n_f^{\uparrow} n_f^{\downarrow}$, and Eq. (1) is an AIM. A fundamental quantity is the so-called dynamical Weiss field $\mathcal{G}_0^{-1}(\omega)$, which describes the noninteracting part of the effective model, and it is related to the Anderson parameters $V_{l\sigma}$ and $\varepsilon_{l\sigma}$ by the relation

$$\mathcal{G}_0^{-1}(i\omega_n) = i\omega_n + \mu - \sum_{l=1}^{N_s} \frac{|V_l|^2}{i\omega_n - \varepsilon_l}. \quad (2)$$

Introducing the impurity Green's function $G(\tau) = -(T_{\mathcal{C}} \tau) c^{\dagger}(0)$ and its imaginary-frequency Fourier transform $G(i\omega_n)$, we can extract the impurity self-energy,

$$\Sigma(i\omega_n) = \mathcal{G}_0^{-1}(i\omega_n) - G^{-1}(i\omega_n), \quad (3)$$

which within DMFT coincides with the local component of the lattice self-energy.

The self-consistency equation which establishes the equivalence between the lattice and the impurity models depends on the noninteracting density of states $D(\varepsilon)$ of the original lattice,

$$G(i\omega_n) = \int d\varepsilon \frac{D(\varepsilon)}{i\omega_n + \mu - \varepsilon - \Sigma(i\omega_n)}. \quad (4)$$

For an infinite-coordination Bethe lattice with semicircular density of states of bandwidth $2D$, Eq. (4) reads

$$\mathcal{G}_0^{-1}(i\omega_n) = i\omega_n + \mu - \frac{D^2}{4} G(i\omega_n). \quad (5)$$

A practical solution of DMFT consists of an iterative solution of the impurity model. Starting from a given choice of the Weiss field, the impurity Green's function has to be computed with some "impurity solver." The knowledge of G allows us to compute Σ from which exploiting the self-consistency condition [Eq. (4)], one finds a new Weiss field. The process is then iterated until convergence.

Let us now briefly recall the basic idea behind using ED as an impurity solver in the DMFT context. ED requires a truncation of the sums over l in Eqs. (1) and (5) up to a finite value N_s , the exact hybridization function being recovered in the limit $N_s \rightarrow \infty$. The accuracy of this method thus relies on how closely one can reproduce an infinite- N_s bath with a finite- N_s one. To be concrete, our discretized impurity model reads exactly as Eq. (1), with a small value of N_l . We can view this as a finite number of "sites," each directly hybridized with the impurity, in the so-called "star" geometry.¹³ At every iteration, once \mathcal{G}_0^{-1} is obtained through the self-consistency equation, the new set of Anderson's parameter is obtained through a fitting procedure, where a functional distance between the \mathcal{G}_0^{-1} coming from Eq. (5) and a discretized version is minimized. In this work, we minimize the function

$$\chi = \sum_n W(i\omega_n) |\mathcal{G}_0(i\omega_n) - \mathcal{G}_0^{N_s}(i\omega_n)|, \quad (6)$$

where \mathcal{G}^{N_s} is the inverse of the discretized version of the Weiss field, the norm $|\cdot|$ is the square root of sum of the squares of the differences of the real and imaginary parts, and $W(i\omega_n)$ is a weight function. In this work, we take the flat function $W(i\omega_n) = 1$, but more selective functions can be useful for specific problems. For example, one can give more weight to small frequencies using $W(i\omega_n) = 1/\omega_n$.¹⁴ The truncation error measured by χ is the only systematic error in the ED solution of DMFT. As shown in Ref. 1, χ decreases exponentially by increasing the number of levels N_s , so that relatively small numbers provide accurate information. The method is also able to provide real-frequency quantities without the need of analytical continuation tools, even if the spectra are necessarily discrete due to the discreteness of the effective model. Nevertheless, much information about single particle and optical spectra can be obtained, mainly as far as the evolution of spectral weight is concerned.¹⁵

In order to access finite temperature properties, one needs in principle the full spectrum of the system. Therefore, the size of the matrix to be diagonalized ($4^{N_s+1} \times 4^{N_s+1}$) poses severe limitations on the values of N_s which can be handled. Even using all the symmetries of the Hamiltonian, one can hardly go beyond $N_s = 5, 6$ using full diagonalization. According to Eq. (5), when self-consistency is achieved, the hybridization function of the bath is proportional to the local Green's function for a Bethe lattice. Therefore, a rough approximation of the bath for small N_s is equivalent to a poor description of $G(i\omega)$.¹⁶ This is expected to be more relevant at low temperature, where the Green's function is more structured, while at high temperature, some structures can be broadened and eventually washed out. Notice that, nonetheless, the value of the energies of the Anderson impurity model can adjust and, in particular, their value can become arbitrarily small, as well as the weights can vanish. In this way, the method is able to describe, e.g., the Mott transition, where the Fermi-liquid coherence energy goes to zero. It is therefore desirable to increase N_s in order to obtain a reliable description of the low-temperature region. A standard way to increase N_s is to replace a full diagonalization with the Lanczos algorithm.¹⁷ In this method, one builds an orthonormal basis in the subspace spanned by the vectors $|\phi\rangle, H|\phi\rangle, H^2|\phi\rangle, \dots, H^{N_l}|\phi\rangle$, where $|\phi\rangle$ is an arbitrary initial state with nonzero overlap to the ground state. One can see that in this basis, the Hamiltonian becomes tridiagonal and that even severely truncating the basis (i.e., limiting the number of states in the Lanczos basis N_l), the lowest-lying states converge to the exact ones very quickly as a function of N_l . In practice, the ground state is very well converged already for basis of the order of $N_l \sim 100$ even for huge matrices of size of the order of millions. Further increasing N_l , the low-lying excited states gradually converge with a speed which basically depends on the energy distance between those states. More care has to be taken to properly handle degenerate states and their multiplicity, as we briefly discuss in Sec. I B.

Due to these convergence properties, this method has been up to now used mainly for the investigation of zero-

temperature properties, for which only the ground state vector needs to be determined. Nevertheless, Lanczos diagonalization can in principle still be used at finite (but low enough) temperatures, for which just a few low-lying states are needed to describe the system. In this work, we demonstrate that such an extension of the Lanczos algorithm can be used successfully in the DMFT context. The next section describes our approach.

A. Extension to finite temperature

As we anticipated previously, we present here a rather straightforward extension of the Lanczos scheme to finite temperature, in which a small number of excited states of the Hamiltonian matrix are computed.

We first show that the relevant quantities of the AIM can be expressed as a sum over the eigenstates of the Hamiltonian, each with a Boltzmann factor which weighs it according to the energy distance from the ground state. Thus, the sums can be truncated to a finite number at low-enough temperatures. This observation is trivial for the partition function $Z = \sum_n e^{-\beta E_n}$. For the impurity Green's function, we start from the usual spectral representation,

$$G_\sigma(i\omega_n) = \frac{1}{Z} \sum_{m,n} \frac{|\langle m | f_\sigma^\dagger | n \rangle|^2}{E_m - E_n - i\omega_n} [e^{-\beta E_n} + e^{-\beta E_m}], \quad (7)$$

in which $|n\rangle$ and E_n are eigenvectors and eigenvalues of H_{AIM} . This can be recast in the form

$$G_\sigma(i\omega_n) = \frac{1}{Z} \sum_m e^{-\beta E_m} G_\sigma^{(m)}(i\omega_n), \quad (8)$$

where

$$G_\sigma^{(m)}(i\omega_n) \equiv \sum_n \frac{|\langle n | f_\sigma | m \rangle|^2}{E_m - E_n - i\omega_n} + \sum_n \frac{|\langle n | f_\sigma^\dagger | m \rangle|^2}{E_n - E_m - i\omega_n}. \quad (9)$$

The ‘‘partial’’ Green's function $G_\sigma^{(m)}(i\omega_n)$ involves creating (or destroying) a particle into state $|m\rangle$. It can be readily calculated from $|m\rangle$ alone, without knowing the whole spectrum spanned by $|n\rangle$, just like the $T=0$ Green's function [which is simply $G_\sigma^{(0)}(i\omega_n)$] can be computed from the ground state.¹⁸ The exponential factor in Eq. (8) indicates that at large enough β only a small number of eigenstates needs to be calculated, and the sums can be limited up to $n = N_{kept}$. Every other spectral quantity, e.g., the dynamical spin susceptibility, can be cast in an analogous form exploiting the Lehmann spectral representation.

The calculation of a few excited states (and hence investigating very low temperatures) is obviously possible, even if it is not as straightforward as the evaluation of the pure ground state. What is far less obvious is whether a reasonably manageable number of states is enough to access the temperature range in which the physical properties of the system start to deviate significantly from $T=0$ (e.g., reaching the Fermi-liquid coherence scale in the correlated metal). The answer to this question depends on the model and on the range of parameters since it is mainly connected with the level spacing in each subsector with given quantum numbers.

In this work, we address this question using as a benchmark test the half-filled Hubbard model. This amounts to iteratively solve the AIM [Eq. (1)], computing the Green's function, and determine from it a new set of parameters ε_l and V_l by minimizing the difference between the two members of Eq. (5). Then the new AIM is solved and the procedure is iterated until convergence.

We demonstrate that the finite- T Lanczos procedure can be applied quite successfully to the investigation of the Mott transition region at finite temperature. Our main results are the following. (i) The method allows us to easily solve the model for $N_s=6$ at a considerably lower computational cost than full diagonalization. (ii) Within finite- T Lanczos, larger values of N_s ($N_s=8,9$ and in principle the same values that are accessible at $T=0$) can be used, which require a huge computational effort using the standard full ED, where the Hamiltonian is fully diagonalized. (iii) Using $N_s=8$, we can draw the phase diagram of the Mott transition up to temperatures close to the Mott transition point at a reasonable computational cost (i.e., keeping a relatively small number of states).

We finally briefly comment on the difference between our use at finite temperature of the standard Lanczos algorithm and the well established finite-temperature Lanczos method developed by Jaklic and Prelovsek.¹¹ The method discussed in Refs. 11 and 12 is an ingenious modification of the Lanczos algorithm, in which the thermal averages are obtained as averages over random samples of shortened Lanczos chains. The original version of the method¹¹ provides remarkably good results in the relatively high-temperature regime, but it is not particularly efficient at low temperatures, and modifications have been proposed to overcome this limitation.¹² On the other hand, our method is precisely built to provide basically exact results for low temperature, and it certainly breaks down (or becomes infeasible) at some temperature. Thus, the two approaches are basically complementary.

B. Control of the approximation

Since the main limitation of the Lanczos method comes from memory requirements, our finite- T implementation can in principle solve matrices of the same size as for $T=0$. In practice, the evaluation of excited states naturally slows down the method, ultimately limiting the number of states we can handle. Notice that the computation of excited states does not only require a larger number of Lanczos steps, but it is further plagued by a loss of orthogonality in the Lanczos basis, which gives rise to the so-called ‘‘ghost states,’’ i.e., to replicas of the converged vectors with small weight. Different procedures have been devised to overcome this problem, mainly based on selective reorthogonalization.¹⁷ This necessary complication of the algorithm leads to an increase of computational time, which depends on many details of the spectrum.

We finally mention a potential limitation of the present approach, which descends from the relative capability of the Lanczos method to handle degenerate states. It is not difficult to realize that if the matrix we try to diagonalize has a degenerate spectrum, the algorithm is not able to separate the

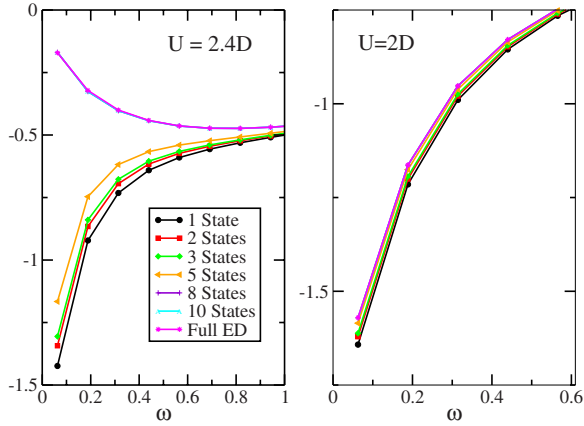


FIG. 1. (Color online) Imaginary part of the local Green's function on the Matsubara axis for different values of N_{kept} compared with the full diagonalization of the Hamiltonian matrix for $N_s=6$ and $\beta=50/D$. The left panel shows $U=2.4D$ and the right one $U=2D$.

different states and to properly determine the multiplicity. The simplest way to avoid this problem is to implement all the symmetries of the Hamiltonian and to diagonalize independently the Hamiltonian matrix in each symmetry subsector. In this case, all the degeneracies associated with those symmetries cannot plague the calculation, as the degenerate states will appear in separated subsectors. Therefore, only the errors arising from accidental degeneracies can affect the accuracy of our calculation. At least in the case we discuss here, we hardly encounter any measurable effect of such degeneracies, even if we cannot completely rule out such effects in other models.

Our approach has two sources of error, whose effects can be minimized in a partially conflicting way. The first is the standard discretization of the Weiss fields, measured by the value of the distance χ defined in Eq. (6), which is more relevant for low temperature, and the second is the truncation in Eq. (7), which will obviously be more and more relevant as T is increased.

We start by discussing the effect of the second kind of truncation since the first has been already discussed in the literature, and it has been shown to be rather benign.¹ We show results for the paramagnetic half-filled Hubbard model, and we compare $G(i\omega_n)$ (we drop henceforth the spin index) obtained from full diagonalization of the Hamiltonian matrix for $N_s=6$, which is basically the maximum size which can be treated with full ED, with our results for different values of N_{kept} for a relatively high temperature $T=1/\beta=1/50$. It is important to underline that N_{kept} is the total number of states in the full Hilbert space. Obviously, the states will belong to different subsectors with given quantum numbers. This means that in each subsector the number of converged states will be significantly smaller, hence the calculation relatively fast. The comparison, reported in Fig. 1, clearly shows that the convergence of our method as a function of N_{kept} is extremely fast, and the results are indistinguishable from the exact ones already for $N_{kept}=10-20$. Lowering the number of kept states, the result approaches the $T=0$ one. We notice

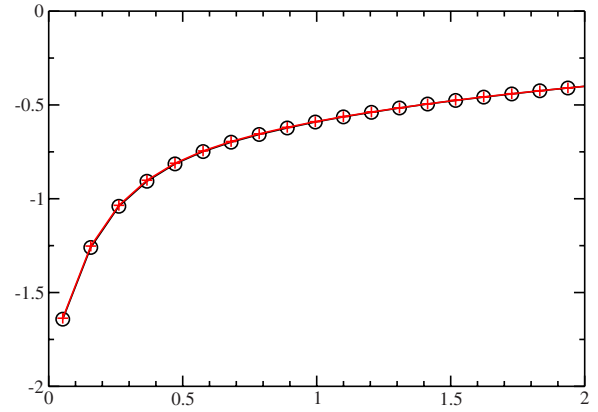


FIG. 2. (Color online) Imaginary part of the local Green's function on the Matsubara axis from finite- T ED ($N_s=8$ and $N_{kept}=40$) and Hirsch-Fye QMC (Ref. 19) for $\beta=60$ and $U=2D$.

that the results converge fast to the exact ones irrespective of the value of the interaction, even in a “difficult” case such as $U=2.4D$, for which the $T=0$ solution is a metal while the system is insulating at $T=1/50$ (convergence is much smoother at, e.g., $U=2.0D$). The inclusion of a few excited states is therefore enough to qualitatively modify the physics of the system. It is important to emphasize the significantly lower computational time of our method, in comparison to the full diagonalization. In our implementation of the selective reorthogonalization, we gain a factor of ~ 10 for $N_{kept}=20$ and ~ 20 for $N_{kept}=10$ with respect to full diagonalization (the precise numbers depend on many details of the spectrum). In practice, the method only introduces a factor of around 3 for $N_{kept}=20$ in the computational time with respect to $T=0$ ED, so it still substantially faster than QMC methods. This benchmark of our approach allows us also to determine a criterion for stopping the inclusion of excited state. We define a “difference” introduced by the inclusion of the n th state, as $D_n = \sum_{i\omega_n} |G^n - G^{n-1}|$ [G^n being the Green's function obtained by including $N_{kept}=n$ states, i.e., n terms in the sum in Eq. (8)] and stop when this distance becomes smaller than a given tolerance, whose value can be extracted from the comparison with full ED for $N_s \leq 6$ and exported to larger N_s values where the full ED is not feasible. This is a first indication that perfectly affordable calculations provide essentially exact results from $T=0$ up to finite temperatures of physical interest. In particular, we used our method for $N_s=8$, where the size of the Hilbert space inhibits, or makes extremely heavy, the full diagonalization of the Hamiltonian. The results, reported in Fig. 2, are definitely satisfactory. The Green's function obtained with our method for $U=2D$, $\beta=60$, and $N_{kept}=40$ is basically indistinguishable from QMC solution for the same physical parameters.

II. RESULTS

In order to prove that our algorithm works in a wide range of parameters, we now draw a phase diagram for $N_s=8$ and $N_{kept}=40$. This relatively high number of excited state has been chosen according to the criterion discussed previously.

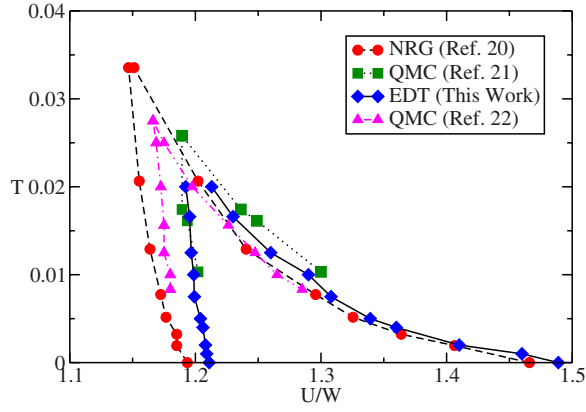


FIG. 3. (Color online) Phase diagram for the Mott transition in the paramagnetic sector obtained through finite-temperature ED with $N_s=8$ and $N_{kept}=40$, compared with previous estimates by numerical renormalization group of Ref. 20 and quantum Monte Carlo of Refs. 21 and 22. The ED curves are stopped at the highest temperature where the chosen number of states determined a negligible truncation error.

More precisely, we obtain $D_{40} < 10^{-8}$ for the highest temperature we consider, $T=0.02W$, and obviously even smaller values for the lower temperatures. We notice that a larger number of states has to be used here with respect to $N_s=6$ due to the larger Hilbert space. The scenario for the Mott transition in the paramagnetic sector in the Hubbard model is now well established. Two distinct solutions exist, with metallic and insulating characters. The former exists for U smaller than a temperature-dependent value $U_{c2}(T)$, and the latter for $U > U_{c1}(T)$. At $T=0$, the transition is of second order and takes place at $U=U_{c2}(0)$, while it becomes of first order at finite temperature. The coexistence region $U_{c1} < U < U_{c2}$ shrinks as the temperature is increased and closes at a critical temperature T_c , where the first-order line ends in a critical point. From a practical point of view, it turns out easier to determine the numerical value of $U_{c2}(T)$ line by computing the local spin susceptibility, a quantity which dramatically changes at the transition point from a Pauli-like susceptibility in the metal to a large ($\propto 1/T$) value associated with local moments in the insulator. This is physically related to the increase of the effective mass when the metallic behavior is lost. The characterization of $U_{c1}(T)$ requires more care. While, like $U_{c2}(T)$, this line is associated with the disappearance of a metastable solution, there is no obvious quantity with a critical behavior when this line is approached. In practice, at each β , we moved from large to small U with extremely small steps until the insulating solution disappears. Figure 3 presents our results for this phase diagram, and a comparison with the numerical renormalization group results of Ref. 20 and the QMC results of Refs. 21 and 22, which are used as references of popular methods used to study the Mott transition. We did not add the results of other approaches (self-energy functional, continuous-time Monte Carlo, etc.) in order to make the figure more readable, and we emphasize that the aim of this comparison is to prove the ability of our approach to study finite-temperature properties accurately rather than a detailed comparison with dif-

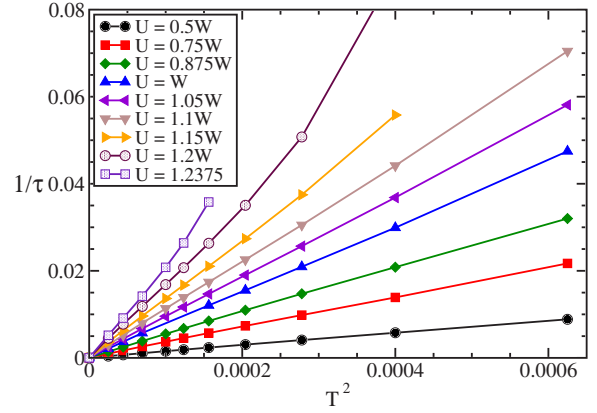


FIG. 4. (Color online) Inverse quasiparticle lifetime $1/\tau$ for $N_s=7$ as a function of square temperature for the displayed values of the correlation strengths. The linear behavior in T^2 characteristic of the Fermi liquid is apparent, with a slope that increases with U/W .

ferent approaches. The reported data clearly show that our method not only reproduces the Mott transition scenario at a qualitative level but also provides results in extremely good quantitative agreement with established methods. In particular, our method is extremely close to NRG at low temperatures, where this approach is basically exact, and it is in very good agreement with QMC at higher temperature, where the latter method becomes accurate. Our method therefore accurately bridges between the most popular well established impurity solvers and allows us to span a sizable region of the phase diagram with good accuracy with a single approach. We find that $N_{kept}=40$ produces a negligible truncation error up to $\beta=50$, where our solution is still in extremely good agreement with previous results. Unfortunately, it is apparently difficult to get closer to the Mott endpoint, where the number of states needed to get a reasonable accuracy becomes larger and larger due to the critical fluctuations which tend to diverge as the critical point is approached. In principle, one gets a Mott endpoint also with 40 states, but the large truncation error suggests us not to plot the data around this point, where the method becomes less reliable, at least quantitatively.

A confirmation of the ability of our method to accurately describe the low-temperature regime, we calculated the inverse lifetime of the quasiparticles $1/\tau = Z_{qp} \lim_{\omega \rightarrow 0} \text{Im} \tilde{\Sigma}(i\omega)$, where $Z_{qp} = [1 - \partial \text{Re} \Sigma(\omega) / \partial \omega]^{-1}$ is the quasiparticle weight. It has been shown that the metallic phase of the Hubbard model studied in DMFT is a Fermi liquid. According to Landau Fermi-liquid theory, $1/\tau$ has to be proportional to T^2 at low temperatures, with a coefficient which increases as we approach the Mott transition. Our method correctly reproduces this behavior with limited computational effort, as shown in Fig. 4. This result is not easily accessible to standard methods, and it shows precisely the main virtue of our approach, which works at its best in the low-temperature regime, where Fermi-liquid behavior and possible violations are directly and unambiguously detectable.

III. CONCLUSIONS

We have shown that a finite-temperature extension of the Lanczos algorithm can be successfully applied to the solution of the self-consistent impurity model appearing in DMFT. The inclusion of a few excited states allows for a reliable description of the physics up to temperatures of the order of the Mott critical endpoint with a relatively small increase of computational cost with respect to the well-established $T=0$ exact diagonalization. The method allows for a computationally cheap investigation of single-band models with extreme accuracy at very low temperatures, where the Fermi-liquid behavior and its possible violations can be investigated unambiguously. Furthermore, the present approach opens the way to the use of ED as a (small) finite-temperature solver for more timely lines of researches, such as cluster extensions of the DMFT^{23,24} and/or realistic calculations of properties of correlated materials,² at basically the same computational cost of $T=0$ studies. As we already discussed, the present algorithm has indeed the same memory requirements as the $T=0$ standard approach

We notice that despite the scaling of ED methods with the number of orbitals (or equivalently, sites in the cluster) is not favorable, ED has been successfully applied at $T=0$ to three-orbital models²⁵ and to CDMFT for a 2×2 plaquette.²⁶ These implementations require a total number of levels of the order of $N_s \approx 12$. As we discussed in Sec. I B, the present

approach can be applied to the same size of matrices (i.e., to the same values of N_s) accessible to the $T=0$ method, and the only limitation is given by the computational time that grows in order to obtain accurate excited states. The actual increase of total time will depend on the temperature and on the size of the system, but our results for $N_s=8$, where the increase factor is around 3 for a range of temperatures that approaches the Mott transition endpoint, are quite promising. We believe anyway that the main use of this approach for multiorbital or cluster models can be to elucidate the really small temperature range, which is never easy to capture with other impurity solvers in the DMFT framework. This range is reasonably accessible with an affordable increase of computational time for the largest systems used in CDMFT and multiorbital DMFT.

ACKNOWLEDGMENTS

We thank J. Tomczak and S. Biermann for discussions and for the QMC data shown in Fig. 3 and N. Blümer for kindly providing us with the data of Ref. 22. M.C. gratefully thanks the hospitality of École Polytechnique, where this work has been mainly carried out and discussions with E. Koch. This work has been partially sponsored by CNR-INFN, MIUR PRIN Prot. 200522492, CNRS-France, and École Polytechnique.

*Present address: Department of Physics and Center for Materials Theory, Rutgers University, Piscataway, New Jersey 08854, USA.

¹For a review, see e.g., A. Georges, G. Kotliar, W. Krauth, and M. J. Rozenberg, *Rev. Mod. Phys.* **68**, 13 (1996).

²For reviews, see e.g., K. Held, I. A. Nekrasov, N. Blümer, V. I. Anisimov, and D. Vollhardt, *Int. J. Mod. Phys. B* **15**, 2611 (2001); A. Georges, in *Lectures on the Physics of Highly Correlated Electron Systems*, edited by A. Avella and F. Mancini (American Institute of Physics, New York, 2004); G. Kotliar, S. Savrasov, K. Haule, V. Oudovenko, O. Parcollet, and C. Marianetti, *Rev. Mod. Phys.* **78**, 865 (2006).

³A. Georges and G. Kotliar, *Phys. Rev. B* **45**, 6479 (1992).

⁴M. Caffarel and W. Krauth, *Phys. Rev. Lett.* **72**, 1545 (1994).

⁵J. E. Hirsch and R. M. Fye, *Phys. Rev. Lett.* **56**, 2521 (1986).

⁶A. N. Rubtsov, V. V. Savkin, and A. I. Lichtenstein, *Phys. Rev. B* **72**, 035122 (2005); P. Werner, A. Comanac, L. de' Medici, M. Troyer, and A. J. Millis, *Phys. Rev. Lett.* **97**, 076405 (2006).

⁷R. Bulla, *Phys. Rev. Lett.* **83**, 136 (1999).

⁸T. Pruschke, M. Jarrell, and J. Freericks, *Adv. Phys.* **42**, 187 (1995).

⁹S. Florens and A. Georges, *Phys. Rev. B* **66**, 165111 (2002).

¹⁰M. Potthoff, *Eur. Phys. J. B* **32**, 429 (2003).

¹¹J. Jaklic and P. Prelovsek, *Phys. Rev. B* **49**, 5065 (1994); *Adv. Phys.* **49**, 1 (2000).

¹²M. Aichhorn, M. Daghofer, H. G. Evertz, and W. von der Linden, *Phys. Rev. B* **67**, 161103(R) (2003).

¹³The noninteracting bath can be parametrized in equivalent alternative ways, as discussed in Ref. 1.

¹⁴M. Capone, M. Civelli, S. S. Kancharla, C. Castellani, and G. Kotliar, *Phys. Rev. B* **69**, 195105 (2004).

¹⁵For a recent calculation of optical properties of the Hubbard model see A. Toschi, M. Capone, M. Ortolani, P. Calvani, S. Lupi, and C. Castellani, *Phys. Rev. Lett.* **95**, 097002 (2005).

¹⁶The linear proportionality between the hybridization function $\Delta(i\omega_n)$ [left-hand side term of Eq. (5)] and $G(i\omega_n)$ holds only for the Bethe lattice, but in generic lattices, the former quantity is a given function of the latter, so that a more structured G reflects in a similar property for Δ .

¹⁷G. H. Golub and C. F. Van Loan, *Matrix Computations* (John Hopkins University Press, Baltimore, 1993).

¹⁸ $G^{(m)}$ is obtained as a continuous fraction with coefficients determined from the Lanczos procedure starting from the vector $f_\sigma^\dagger|m\rangle$ (or $f_\sigma|m\rangle$).

¹⁹J. M. Tomczak (private communication).

²⁰R. Bulla, T. A. Costi, and D. Vollhardt, *Phys. Rev. B* **64**, 045103 (2001).

²¹J. Joo and V. Oudovenko, *Phys. Rev. B* **64**, 193102 (2001).

²²N. Blümer, Ph.D. thesis, Universität Augsburg, 2002.

²³G. Kotliar, S. Y. Savrasov, G. Palsson, and G. Biroli, *Phys. Rev. Lett.* **87**, 186401 (2001).

²⁴T. Mauer, M. Jarrell, T. Pruschke, and J. Keller, *Eur. Phys. J. B* **13**, 613 (2000); M. H. Hettler, A. N. Tahvildar-Zadeh, M. Jarrell, T. Pruschke, and H. R. Krishnamurthy, *Phys. Rev. B* **58**, R7475 (1998).

²⁵M. Capone, M. Fabrizio, C. Castellani, and E. Tosatti, *Science* **296**, 2364 (2002); *Phys. Rev. Lett.* **93**, 047001 (2004).

²⁶M. Civelli, M. Capone, S. S. Kancharla, O. Parcollet, and G. Kotliar, *Phys. Rev. Lett.* **95**, 106402 (2005); B. Kyung, S. S. Kancharla, D. Sénéchal, A.-M. S. Tremblay, M. Civelli, and G. Kotliar, *Phys. Rev. B* **73**, 165114 (2006).